Inflammation and skin cholesterol in LDLr$^{-/-}$, apoA-I$^{-/-}$ mice: link between cholesterol homeostasis and self-tolerance?

Manal Zabalawi,[*,†] Manish Bharadwaj,[*,†] Heather Horton,[*,†] Mark Cline,[†] Mark Willingham,[†] Michael J. Thomas,[§] and Mary G. Sorci-Thomas[1,*,†,§]

Lipid Sciences Research Center,* and Departments of Pathology,† and Biochemistry,§ Wake Forest University Medical Center, Winston-Salem, NC 27157

Abstract **Diet-fed low density lipoprotein receptor-deficient/apolipoprotein A-I-deficient (LDLr$^{-/-}$, apoA-I$^{-/-}$) mice accumulate a 10-fold greater mass of cholesterol in their skin despite a 1.5- to 2-fold lower plasma cholesterol concentration compared with diet-fed LDLr$^{-/-}$ mice. The accumulation of cholesterol predominantly in the skin has been shown to occur in a growing number of other hypercholesterolemic double knockout mouse models sharing deficits in genes regulating cellular cholesterol homeostasis. Exploring the relationship between cholesterol balance and inflammation, we have examined the time course of cholesterol accumulation in a number of extrahepatic tissues and correlated with the onset of inflammation in diet-fed LDLr$^{-/-}$, apoA-I$^{-/-}$ mice. After 4 weeks of diet, LDLr$^{-/-}$, apoA-I$^{-/-}$ mice showed a significant increase in skin cholesterol mass compared with LDLr$^{-/-}$ mice. In addition, after 4 weeks on the diet, cholesterol accumulation in the skin was also found to be associated with macrophage infiltration and accompanied by increases in tumor necrosis factor-α, cyclooxygenase-2, and langerin mRNA, which were not seen in the liver. Overall, these data suggest that as early as 4 weeks after starting the diet, the accumulation of skin cholesterol and the onset of inflammation occur concurrently. In summary, the use of hypercholesterolemic LDLr$^{-/-}$, apoA-I$^{-/-}$ mice may provide a useful tool to investigate the role that apoA-I plays in maintaining cholesterol homeostasis and its relationship to inflammation.—**Zabalawi, M., M. Bharadwaj, H. Horton, M. Cline, M. Willingham, M. J. Thomas, and M. G. Sorci-Thomas. **Inflammation and skin cholesterol in LDLr$^{-/-}$, apoA-I$^{-/-}$ mice: link between cholesterol homeostasis and self-tolerance?** *J. Lipid Res.* **2007.** 48: **52–65.**

Supplementary key words apolipoprotein A-I • high density lipoprotein • inflammation • low density lipoprotein receptor-deficient/apolipoprotein A-I-deficient mice • whole body cholesterol • skin • itch

The plasma HDL apolipoprotein A-I (apoA-I) concentration is a powerful inverse correlate of atherosclerosis risk in humans (1). The most prominent mechanism explaining its atheroprotective role is through the directional movement of peripheral tissue cholesterol to the liver via a pathway referred to as "reverse cholesterol transport." This pathway describes a mechanism of cholesterol removal and was first proposed by Glomset and Norum (2). Excess cholesterol is removed from peripheral tissues and cells organized by apoA-I into phospholipid complexes, then transported to the liver for excretion. A number of steps have been shown to be critical in completing the overall pathway (3). In vivo studies aimed at establishing the role of HDL apoA-I as the main physiological efflux acceptor of peripheral tissue cholesterol have shown that the absence of apoA-I has little or no effect on centripetal cholesterol transport, suggesting that the movement of peripheral tissue cholesterol via HDL apoA-I is not a rate-limiting step in net cholesterol removal (4–7).

In other studies, the role of apoA-I in reverse cholesterol transport has been tested with specific emphasis on macrophage cholesterol and not peripheral tissue cholesterol efflux. In one report (8), apoA-I was found to inhibit foam cell formation in apoE knockout mice after monocyte adherence to endothelium. In another study, mice deficient in both apoE and apoA-I but expressing macrophage-derived apoE were found to have 2- to 3-fold lower plasma cholesterol than mice deficient in only apoE and expressing macrophage apoE. In spite of the lower plasma cholesterol, the apoA-I and apoE double knockout mice had atherosclerotic lesions 60% larger than in the apoE only knockout mice expressing macrophage apoE (9). More recently, using a method of monitoring the in vivo fate of radiolabeled macrophage cholesterol, a study showed that overexpression of liver-derived apoA-I promotes reverse cholesterol transport from macrophages to feces more efficiently than in mice with normal levels of plasma apoA-I (10). Using the same method, liver-

Manuscript received 17 August 2006 and in revised form 12 October 2006.
Published, JLR Papers in Press, October 28, 2006.
DOI 10.1194/jlr.M600370-JLR200

[1] To whom correspondence should be addressed.
e-mail: msthomas@wfubmc.edu

expressed scavenger receptor class B type I was also shown to be essential for reverse cholesterol transport (11). Thus, these studies suggest that although macrophage cholesterol efflux contributes little to the plasma concentration of HDL, macrophage cholesterol efflux to apoA-I is highly important in preventing foam cell formation and in stimulating the transport and excretion of cholesterol from the body (12, 13).

In addition to apoA-I's role in cholesterol transport and removal, increasing evidence supports its function as an important inhibitor of cellular inflammation. A large body of evidence suggests that inflammatory mechanisms mediate the initiation and development of atherosclerosis (14–16) as well as inhibit the onset of inflammation by blocking the formation of oxidized LDL and, thus, the stimulation of macrophages into foam cells. The possible mechanisms linking apoA-I's role in cholesterol removal and its role as an anti-inflammatory mediator have not been fully elucidated. These questions prompted the current studies in diet-fed low density lipoprotein receptor-deficient/apolipoprotein A-I-deficient ($LDLr^{-/-}$, $apoA\text{-}I^{-/-}$) double knockout mice, in which whole animal and tissue cholesterol balance was studied as a function of time and its relationship to inflammation was also studied.

In our efforts to elucidate the role of apoA-I in protecting against the development of atherosclerosis, we used the diet-fed $LDLr^{-/-}$, $apoA\text{-}I^{-/-}$ mouse model. Previous studies from our laboratory (17) and by others (18, 19) have shown that this and similar apoA-I-deficient mouse models are useful for studying the links between cholesterol homeostasis and inflammation.

MATERIALS AND METHODS

Mice and experimental diet

$LDLr^{-/-}$, $apoA\text{-}I^{-/-}$, and $LDLr^{-/-}$, $apoA\text{-}I^{-/-}$ mice were housed at the Wake Forest University Medical Center, where procedures were approved by the Animal Care and Use Committee of the Wake Forest University Health Sciences and in accordance with Public Health Service guidelines. All genotypes of mice were fully crossed (more than nine generations) into the C57BL/6 background, as described previously (17).

At 6 weeks of age, mice were fed a diet as described previously (17), consisting of 10% of energy as fat, with the fatty acid composition as described previously (20, 21) for palm or safflower oil, and the cholesterol content was set at 0.1%. As controls, both gender- and aged-matched mice of each genotype were fed a Purina chow diet for 16 weeks. All mice were maintained in a temperature-controlled room with a 12 h light/12 h dark cycle. Both genotypes of mice were observed to consume an equal amount of diet during the study period; thus, no significant differences were found when body weights between different genotypes of like gender were compared.

At the end of the diet period, both chow- and diet-fed mice were fasted for 2–3 h and then anesthetized, and blood was obtained by cardiac puncture. Because of the serious skin lesions that developed in diet-fed $LDLr^{-/-}$, $apoA\text{-}I^{-/-}$ double knockout mice, some animals, particularly female mice, were euthanized before the 16 week length of the study, usually at ~12 weeks. In those cases, an equivalent number of diet-fed $LDLr^{-/-}$ mice were also euthanized at that time point. Approximately 1 ml of blood was collected in a 1.5 ml tube containing 20 μl of 0.5 μM EDTA, pH 8.0, and 1 μM sodium azide and placed immediately on ice. The blood was centrifuged immediately at 4°C at 10,000 rpm for 10 min. The plasma was removed and stored at –80°C. The animal was opened via midline laparotomy to expose the thoracic and abdominal cavities, and tissues were immediately removed and frozen in liquid nitrogen or placed in 10% formalin.

Plasma cholesterol, serum amyloid A, and Monocyte chemotactic protein-1analyses

Plasma from both chow- and diet-fed mice was analyzed for total plasma and free and esterified cholesterol (17). Plasma serum amyloid A concentration was measured by ELISA using a kit from Biosource International (Camarillo CA), whereas plasma MCP-1 protein was measured by ELISA using a kit from R&D Systems (Minneapolis, MN).

Tissue lipid analyses

For tissue cholesterol determination, all of the major organs were removed, weighed, and saponified in KOH as described (7), and the remaining carcass was also saponified (6), after which total tissue cholesterol was determined by GC analysis (17). For whole body cholesterol measurements before hydrolysis, any unabsorbed diet in the digestive tract was removed before saponifying the entire animal (including blood) in KOH (22). No significant differences in total organ wet weight between the two diet-fed genotypes was noted in any of the major organs except spleen. By 14–16 weeks of the study, diet-fed $LDLr^{-/-}$, $apoA\text{-}I^{-/-}$ mice showed a 1.5× increase in spleen wet weight compared with diet-fed $LDLr^{-/-}$ mice. This increase in wet weight was not attributable to an accumulation of cholesterol in the spleen, as shown below.

To minimize sampling error for the analysis of skin cholesterol mass, sections of skin from four different anatomically distinct areas were taken from each animal at the time of necropsy and frozen. Samples of whole skin, ~200 mg from each location, were extracted separately and analyzed. Aliquots of the lipid extraction were taken and subjected to GC analysis for free and esterified cholesterol content (17).

The skin phospholipid fatty acid composition was determined as described previously (23, 24). Further analyses of skin cholesterol and phospholipid were performed using mass spectrometry, as described previously (25). In addition, skin F_2-isoprostane mass was determined using previously described methods (26).

Cholesterol determination on resident and thioglycollate-elicited peritoneal macrophages

The free and esterified cholesterol mass was measured from both resident and thioglycollate-elicited peritoneal macrophages from 16 week 0.1% cholesterol + 10% palm oil-fed $LDLr^{-/-}$, $apoA\text{-}I^{-/-}$ and $LDLr^{-/-}$ mice as described previously (27, 28). Peritoneal exudate cells were incubated in plastic dishes for 3–4 h, after which nonadherent cells were discarded. Adherent cells were then extracted for cellular cholesterol directly from the dishes, and their mass was determined by gas-liquid chromatography.

Intestinal cholesterol absorption and bile composition

Cholesterol absorption was measured by the fecal dual-isotope ratio method (29). Chow-fed male mice were dosed intragastrically with a mixture of 2 μCi of [5,6-^{3}H]sitostanol and 1 μCi of [4-^{14}C]cholesterol. Mice were housed individually, and their stools were collected over the following 72 h. Stool samples were extracted, and the ratio of ^{14}C to ^{3}H for each mouse was

determined. The percentage cholesterol absorption was calculated from these data as described previously (29).

Bile was collected from the gallbladder of anesthetized mice using a 30 gauge needle, and total bile cholesterol mass was measured by GC (17); total bile acids were measured enzymatically as described previously (30). Serum bile acid was measured using established methods (31). Aspartate aminotransferase and alanine aminotransferase measurements were conducted at the Wake Forest University Comparative Medicine Pathology Laboratory.

RNA isolation and RT-PCR

RNA was isolated from frozen tissue using Trizol Reagent (Invitrogen) according to the manufacturer's instructions. The concentration of purified RNA was determined by the optical density at 260 nm. For cDNA synthesis, 1 μg of total RNA was used for reverse transcription using random primers (Promega) and the OmniScript RT kit (Qiagen). Real-time quantitative PCR was performed using an Applied Biosystems 7000 sequence detector and the manufacturer's suggestions. For negative controls, reverse transcriptase was omitted at the time of cDNA synthesis to determine the extent of genomic DNA contamination. Primers were created using Primer Express and synthesized by Integrated DNA Technologies (Coralville, IA). All values are relative to GAPDH and normalized to an age-matched chow-fed mouse for the appropriate genotype and tissue using the ΔΔCt method (32). All primer sequences are available upon request.

Histology and immunohistochemistry

Histological sections of liver and skin from chow- and diet-fed mice were fixed with 10% formalin at the end of the study. After fixation, tissues were infiltrated with a 20% sucrose solution overnight at 4°C. Tissues were embedded in Tissue-Tek OCT (Sakura) overnight and sectioned at −25°C. Sections were stained using Oil Red O/Dextrin and counterstained with Mayer's hematoxylin. The slides were examined with a Zeiss Axioplan 2 microscope, and digital images were recorded. Images were then prepared for publication using Adobe Photoshop 7.0.

Rat IgG anti-F4/80 (Serotec) was used as a macrophage marker for formalin-fixed paraffin-embedded sections of skin. Sections were deparaffinized and rehydrated and then treated with 0.1% trypsin for 30 min at 37°C. Sections were blocked with 1% BSA and incubated overnight at 4°C with anti-F4/80 (1:25) followed by incubation with goat anti-rat IgG (1:50) (Jackson ImmunoResearch) for 30 min at 35°C. Sections were treated with streptavidin alkaline phosphatase (Biogenex) at 35°C for 30 min and then the red alkaline phosphatase substrate kit I (Vector), followed by counterstaining with Mayer's hematoxylin.

Data analysis

Data are presented as means ± SEM or means ± SD, as indicated. Data were analyzed by one-way ANOVA using Prism 4.0, and then individual differences between groups were found using Fisher's least significant posthoc test.

RESULTS

Genotype-specific response to dietary fat and cholesterol

LDLr$^{-/-}$, apoA-I$^{-/-}$ and LDLr$^{-/-}$ mice were fed a diet containing 0.1% cholesterol and 10% palm oil for 16 weeks. At various times during the study, blood samples were taken and analyzed for plasma cholesterol concentrations, as shown in **Fig. 1**. Figure 1A, B show the total plasma cholesterol concentrations for LDLr$^{-/-}$, apoA-I$^{-/-}$ and LDLr$^{-/-}$ mice, respectively, during the course of the study. When LDLr$^{-/-}$, apoA-I$^{-/-}$ and LDLr$^{-/-}$ mice were fed chow for 16 weeks similar amounts of total plasma cholesterol, averaging ~220 and ~300 mg/dl, respectively, were observed. However, once the mice were challenged with dietary cholesterol, these two genotypes of mice responded quite differently (17). Although LDLr$^{-/-}$ mice showed a large 5-fold increase in plasma cholesterol in response to diet, the LDLr$^{-/-}$, apoA-I$^{-/-}$ mice showed a more modest 3-fold increase from chow levels. In previously published studies (17), data show that the lipoprotein and apolipoprotein distribution in both genotypes on the chow diet are similar except for the absence of apoA-I-containing HDL-sized particles in the LDLr$^{-/-}$, apoA-I$^{-/-}$ mice. However, in reaction to the cholesterol-containing diet, a genotype-specific response showed that LDLr$^{-/-}$ mice had a more profound increase in VLDL and LDL cholesterol

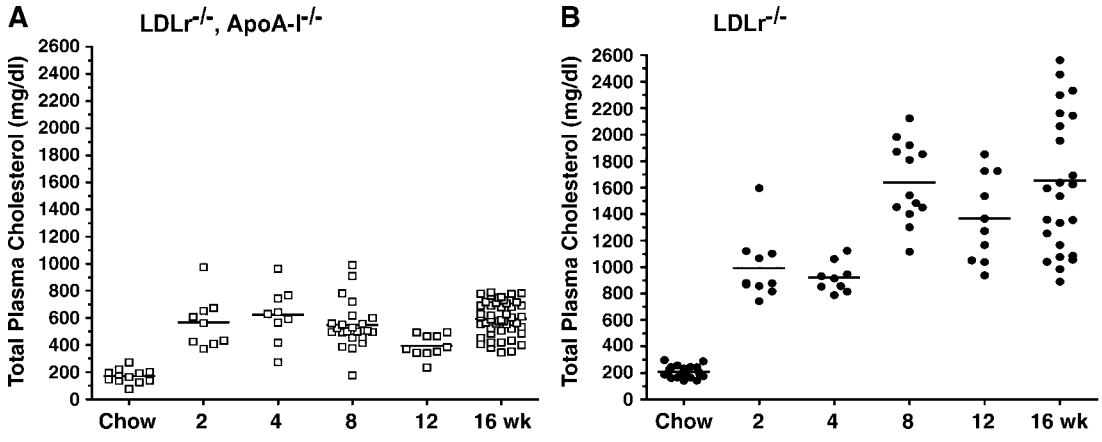

Fig. 1. Differential plasma cholesterol response to dietary cholesterol in low density lipoprotein receptor-deficient/apolipoprotein A-I-deficient (LDLr$^{-/-}$, apoA-I$^{-/-}$) and LDLr$^{-/-}$ mice. Total plasma cholesterol levels are shown for LDLr$^{-/-}$, apoA-I$^{-/-}$ (A) and LDLr$^{-/-}$ (B) mice consuming a 0.1% cholesterol + 10% palm oil diet. The plasma of chow-fed mice was assayed at the 16 week time point only. No significant differences were seen in plasma cholesterol between male and female mice within a genotype at any time point. All values represent means ± the SD of 8–12 male and female mouse plasma samples measured using an enzymatic assay.

concentration than did LDLr$^{-/-}$, apoA-I$^{-/-}$ mice, whereas the diet-fed LDLr$^{-/-}$, apoA-I$^{-/-}$ mice showed a larger increase in lipoprotein triglycerides and apoE content than did LDLr$^{-/-}$ mice (17). In summary, at all time points, the average total plasma cholesterol was ~2.5-fold lower in the diet-fed LDLr$^{-/-}$, apoA-I$^{-/-}$ mice compared with diet-fed LDLr$^{-/-}$ mice, with no significant differences seen between male and female mice within a genotype.

Intestinal cholesterol absorption was similar between genotypes

Given the specific-diet responsiveness in total plasma cholesterol concentration, we hypothesized that in mice lacking apoA-I, intestinal cholesterol absorption might be lower, thus explaining the lower plasma cholesterol seen in this genotype (Fig. 1A vs. B). To address this, we measured intestinal cholesterol absorption using the dual-isotope method; the results are shown in **Fig. 2**. The percent cholesterol absorption was found to be similar in all three different genotypes examined, apoA-I$^{-/-}$, LDLr$^{-/-}$, and LDLr$^{-/-}$, apoA-I$^{-/-}$, with values ranging from 55% to 60%. These results suggest that the genotype-related difference in total plasma cholesterol in response to dietary cholesterol was not related to intestinal cholesterol absorption in the LDLr$^{-/-}$, apoA-I$^{-/-}$ mice.

Accumulation of whole body cholesterol in diet-fed LDLr$^{-/-}$, apoA-I$^{-/-}$ mice

The effects of diet consumption on cholesterol homeostasis was next investigated by measuring total body cholesterol mass in LDLr$^{-/-}$, apoA-I$^{-/-}$ and LDLr$^{-/-}$ mice after 8 and 16 weeks on diet; the results are shown in **Fig. 3**. In agreement with other investigators, 16 week chow-fed mice showed ~200 mg/100 g body weight total cholesterol, regardless of genotype (22). As expected, when diet was administered, both genotypes responded by showing an increase in total cholesterol body mass, which can be accounted for by an increase in plasma and liver cholesterol

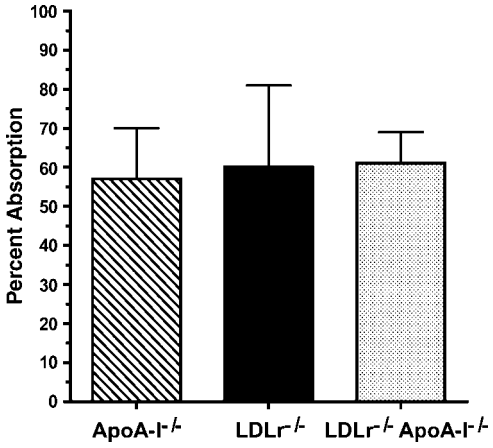

Fig. 2. Intestinal cholesterol absorption in apoA-I$^{-/-}$, LDLr$^{-/-}$, and LDLr$^{-/-}$, apoA-I$^{-/-}$ mice. Cholesterol absorption was measured using the fecal dual-isotope ratio method, as described in Materials and Methods. All values represent means ± SD of five male chow-fed mice per genotype.

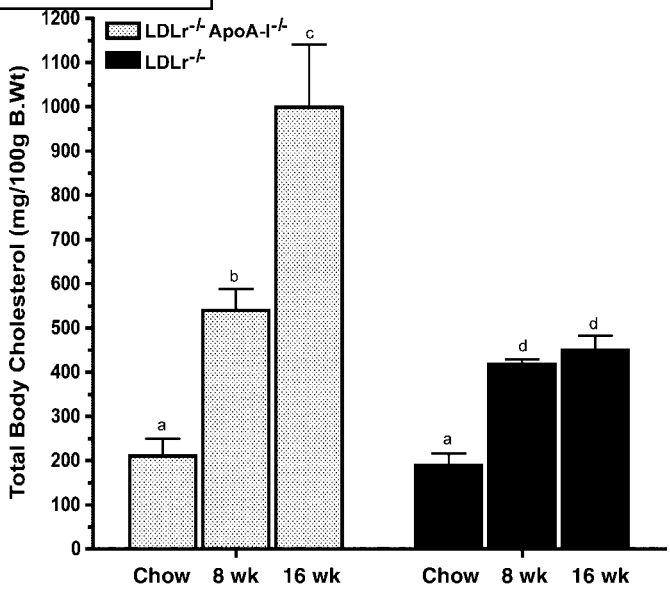

Fig. 3. Whole body cholesterol mass in LDLr$^{-/-}$, apoA-I$^{-/-}$ and LDLr$^{-/-}$ mice. LDLr$^{-/-}$, apoA-I$^{-/-}$ and LDLr$^{-/-}$ mice were fed either chow for 16 weeks or 0.1% cholesterol + 10% palm oil for 8 and 16 weeks. At the indicated times, whole body cholesterol mass was determined as described in Materials and Methods. All values represent means ± SD of three to four male and three to four female mice per genotype. Values with different letters indicate statistically significant differences at $P < 0.01$. No differences in body weight (B.Wt) in like genders between genotypes on either chow or diet were noted. However, significant differences were found between male and female mice within a genotype and when male or female mice were compared from chow to diet within a genotype ($P < 0.05$). Body weights were 20.4 ± 1 (female), 24.8 ± 3 (male) and 21.3 ± 1.5 (female), 25.9 ± 2.3 (male) for 16 week chow-fed LDLr$^{-/-}$, apoA-I$^{-/-}$ and LDLr$^{-/-}$ mice, respectively. Body weights were 22.9 ± 1.3 (female), 26.7 ± 4 (male) and 23.0 ± 1.3 (female), 28.7 ± 2.7 (male) for 16 week diet-fed LDLr$^{-/-}$, apoA-I$^{-/-}$ and LDLr$^{-/-}$ mice, respectively. Based on the data shown here, the average cholesterol mass per mouse was 46 and 44 mg for 16 week chow-fed LDLr$^{-/-}$, apoA-I$^{-/-}$ and LDLr$^{-/-}$ mice, respectively, and 250 and 117 mg for 16 week diet-fed LDLr$^{-/-}$, apoA-I$^{-/-}$ and LDLr$^{-/-}$ mice, respectively.

levels (33). However, by 8 weeks of diet, the LDLr$^{-/-}$, apoA-I$^{-/-}$ mice had accumulated a statistically greater mass of whole body cholesterol than had the LDLr$^{-/-}$ mice, despite their lower total plasma cholesterol levels (Fig. 1). After 16 weeks, the LDLr$^{-/-}$, apoA-I$^{-/-}$ mice had accumulated nearly double the content of whole body cholesterol as LDLr$^{-/-}$ mice fed the same diet. These differences in whole body cholesterol could not be explained by dietary intake as both genotypes were observed to consume equal amounts of diet during the study period; thus, no significant differences were found when body weights between different genotypes of like genders were compared.

Distribution of tissue cholesterol in diet-fed LDLr$^{-/-}$, apoA-I$^{-/-}$ mice

We next sought to determine which tissue(s) showed an overall net increase in cholesterol mass as a result of the accumulation of whole body cholesterol. Again, LDLr$^{-/-}$, apoA-I$^{-/-}$ and LDLr$^{-/-}$ mice were fed the 0.1% choles-

terol, 10% palm oil diet for 16 weeks. At the end of the study, all major peripheral organs were removed and analyzed for their total cholesterol content. **Figure 4A** shows total organ cholesterol levels, expressed as mg cholesterol/g wet weight, for skin, adrenal, lung, kidney, testes, ovary, liver, spleen, brain, adipose, muscle, and intestine; Fig. 4B shows the same data expressed as mg/organ. These results strikingly show that the only significant site of cholesterol accumulation was the skin, whereas cholesterol mass in the adrenal, liver, and spleen was reduced compared with diet-fed LDLr$^{-/-}$ mice. The reduced cholesterol mass in LDLr$^{-/-}$, apoA-I$^{-/-}$ mouse adrenals was similar to that reported in an earlier study (17) and agrees with observations in apoA-I$^{-/-}$ mice (34, 35), which show that deletion of apoA-I severely alters adrenal cholesteryl ester content. Of particular note, the significantly lower cholesterol content in LDLr$^{-/-}$, apoA-I$^{-/-}$ mouse spleen was the result of a significant increase in spleen wet weight in all 16 week diet-fed LDLr$^{-/-}$, apoA-I$^{-/-}$ mice. These mice uniformly showed a 1.5-fold increase in spleen wet weight

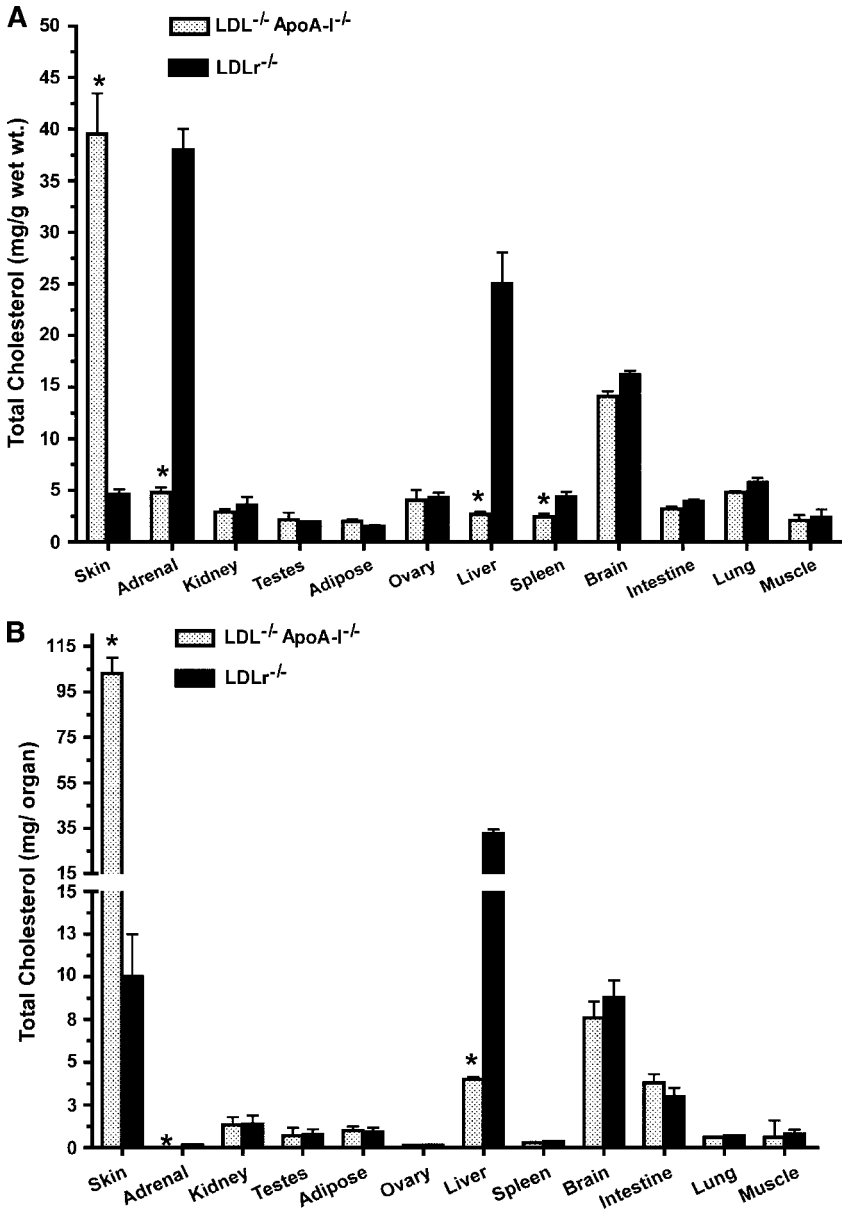

Fig. 4. Peripheral organ cholesterol distribution in LDLr$^{-/-}$, apoA-I$^{-/-}$ and LDLr$^{-/-}$ mice. LDLr$^{-/-}$, apoA-I$^{-/-}$ and LDLr$^{-/-}$ mice were fed a 0.1% cholesterol + 10% palm oil diet for 16 weeks. At the end of the study, tissues were removed and their cholesterol contents determined as described in Materials and Methods. A: Data as mg/g wet weight. B: The same data as mg/organ. All values represent means ± SD of four male and four female mice per genotype. No gender differences in tissue cholesterol mass were noted. Asterisks indicate statistically significant differences between genotypes for skin, adrenal, liver, and spleen at $P < 0.02$ in A and for skin, adrenal, and liver at $P < 0.01$ in B. In rodents, skin accounts for ~11 g per 100 g of body weight.

compared with diet-fed LDLr$^{-/-}$ mice. Thus, this "apparent reduction" in spleen cholesterol mass per wet weight (Fig. 4) was not the result of a depletion in cholesterol mass. Therefore, it should be reemphasized that no other major organ studied showed detectable changes in wet weight compared between genotypes (data not shown). This suggests that the observed decrease in liver cholesterol content in diet-fed LDLr$^{-/-}$, apoA-I$^{-/-}$ mice was in fact a reflection of a decrease in cholesterol mass and not a result of changes in liver wet weight between genotypes. Additionally, as measures of overall liver function, both aspartate aminotransferase and alanine aminotransferase levels were measured in 16 week diet-fed LDLr$^{-/-}$, apoA-I$^{-/-}$ versus LDLr$^{-/-}$ mice and found not to be different between genotypes.

Both the bile cholesterol and bile acid contents from 16 week diet-fed LDLr$^{-/-}$, apoA-I$^{-/-}$ and LDLr$^{-/-}$ mice were also examined. After 16 weeks of diet, the LDLr$^{-/-}$, apoA-I$^{-/-}$ mice showed 6.2 ± 0.1 μg/μl cholesterol in the bile, and LDLr$^{-/-}$mice had 9.2 ± 0.2 μg/μl, possibly reflecting the lower liver cholesterol content. Total gallbladder bile acids were 124 ± 6 μmol/ml in LDLr$^{-/-}$, apoA-I$^{-/-}$ mice and 110 ± 4 μmol/ml in LDLr$^{-/-}$mice, similar to the values reported in other genotypes of diet-fed mice (36, 37). No significant differences were noted in serum bile acid content between genotypes (data not shown).

Liver cholesterol mass decreases with time in diet-fed LDLr$^{-/-}$, apoA-I$^{-/-}$ mice

To more thoroughly investigate the time course of liver cholesterol depletion in the diet-fed LDLr$^{-/-}$, apoA-I$^{-/-}$ mice, additional studies were performed. **Figure 5A, C** show Oil Red O-stained liver sections from LDLr$^{-/-}$ mice fed diet for 2 and 16 weeks, compared with Figure 5B, D, which show Oil Red O-stained liver sections from LDLr$^{-/-}$, apoA-I$^{-/-}$ mice fed diet for 2 and 16 weeks, respectively. These data show that the size and frequency of Oil Red O staining droplets were similar between the two genotypes after 2 weeks on the diet. However, when liver sections from 16 week diet-fed mice were evaluated from each of the two genotypes, the diameters of neutral lipid droplets in LDLr$^{-/-}$ mouse livers were as large as those seen in 2 week livers, whereas lipid droplets observed in the 16 week diet-fed LDLr$^{-/-}$, apoA-I$^{-/-}$ liver sections were significantly smaller (Fig. 5C, D). These images agree well with the mass measurement of liver cholesterol from LDLr$^{-/-}$, apoA-I$^{-/-}$, LDLr$^{-/-}$, and apoA-I$^{-/-}$ mouse livers as a function of time on diet, shown in Fig. 5E. Interestingly, all three genotypes showed similar liver cholesterol content after 16 weeks on chow or after 2 weeks on the diet. However, after ~4 weeks, the diet-fed LDLr$^{-/-}$, apoA-I$^{-/-}$ mice showed a statistically significant decrease in liver cholesterol levels, which was not seen in the other two genotypes (Fig. 5E). Triglyceride mass in the liver was not different between genotypes. Again, the changes in LDLr$^{-/-}$, apoA-I$^{-/-}$ mouse liver total cholesterol were not the result of differences in liver wet weight, as noted previously. Liver wet weights were compared between all LDLr$^{-/-}$, apoA-I$^{-/-}$ and LDLr$^{-/-}$ mice at the time of necropsy, with both genotypes showing total liver weights of ~1.3–1.4 g, with the expected gender-associated weight differences.

Cholesterol accumulates primarily in the skin of LDLr$^{-/-}$, apoA-I$^{-/-}$ mice

We next investigated the time course of cholesterol accumulation in skin and its association with inflammation. In previous studies, we observed that as early as 10–12 weeks after starting the diet, LDLr$^{-/-}$, apoA-I$^{-/-}$ mice developed severe skin lesions that we believed to be attributable to massive cholesterol deposits. From our observations, we noted that once the lesions developed, the mice showed signs of systemic inflammation and eventually died (17). Furthermore, female mice were found to develop lesions earlier than male mice, but with both genders of mice displaying quantitatively equal accumulations of cholesterol mass in the skin (17).

A major question addressed in these studies was the time course of skin cholesterol accumulation, providing a means to more fully investigate the initiating events leading to the accumulation of cholesterol in the skin. Therefore, we measured the mass of cholesterol in mouse skin with time. **Figure 6A** shows a 12 week diet-fed LDLr$^{-/-}$, apoA-I$^{-/-}$ mouse, with the typical thick skin folds accompanied by hair loss and edema associated with the massive accumulation of cholesterol in the skin. The hair loss was associated with an increase in cholesterol mass, as shown in Fig. 6B (similar data were obtained regardless of the type of fat fed). From the mass analyses, we found that diet-fed LDLr$^{-/-}$, apoA-I$^{-/-}$ mice accumulated significantly more cholesterol after 4 weeks on the diet than did diet-fed LDLr$^{-/-}$ mice. The majority of the cholesterol accumulating in the skin was in the form of cholesteryl ester Furthermore, the accumulation of skin cholesterol appeared to be independent of the specific locations from which the sections were taken.

When skin sections were processed for histological evaluation with Oil Red O, neutral lipid deposition was significantly increased by 4 weeks of diet in LDLr$^{-/-}$, apoA-I$^{-/-}$ mouse skin (Fig. 6C) and not in LDLr$^{-/-}$ skin, which showed normal dermal-layer thickness (data not shown). This dramatic thickening of the dermis of diet-fed LDLr$^{-/-}$, apoA-I$^{-/-}$ mouse skin agrees with the statistically significant increase in skin cholesterol mass. With time, the accumulation of the neutral staining cholesteryl ester was accompanied by an increase in dermal thickness, as shown by histological analysis (Fig. 6D) and mass determinations (Fig. 6B). This increase in the deposition of cholesteryl ester in the dermis concurs with the accumulation of cholesterol clefts seen from previously published hematoxylin and eosin-stained sections from 16 week chow- and diet-fed LDLr$^{-/-}$, apoA-I$^{-/-}$ and LDLr$^{-/-}$ mice (17).

The massive cholesterol deposits in the dermis of diet-fed LDLr$^{-/-}$, apoA-I$^{-/-}$ mice were also found to be associated with increased macrophage infiltration and ac-

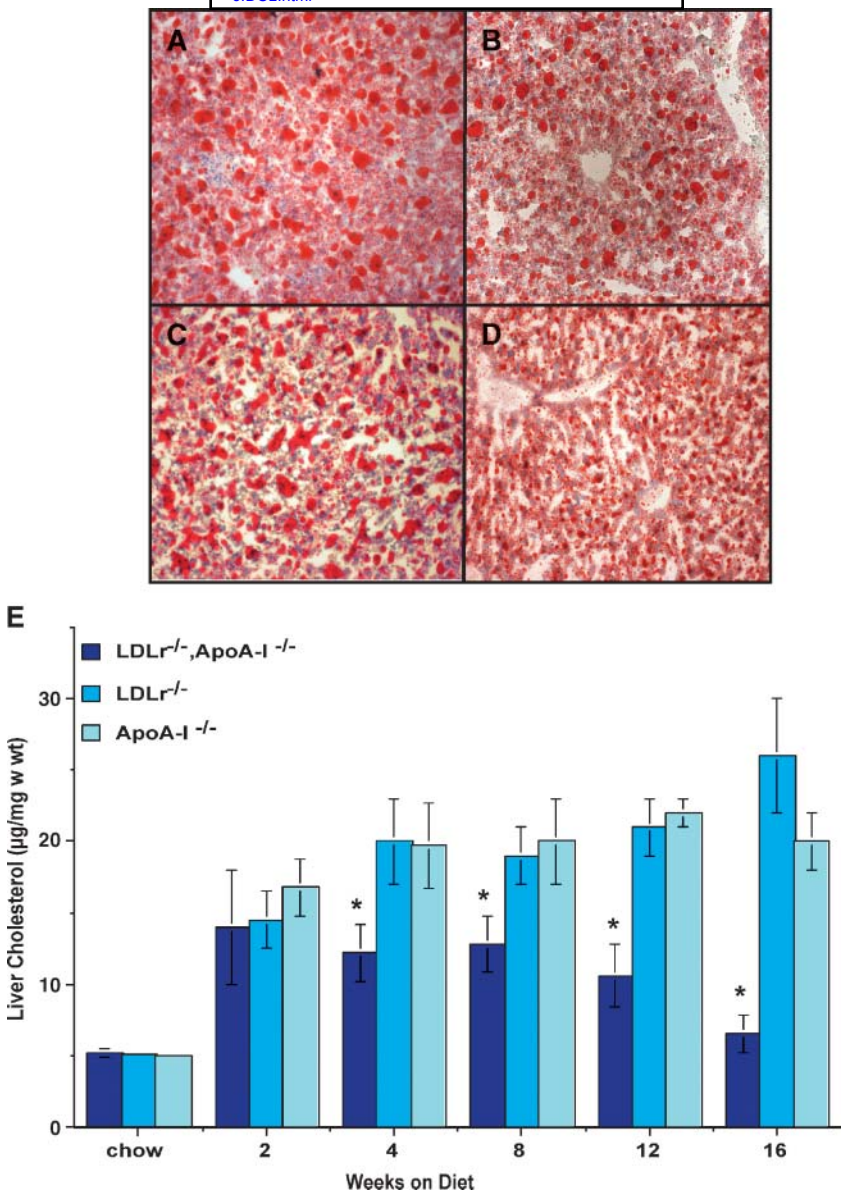

Fig. 5. Time course reduction in liver cholesterol mass in LDLr$^{-/-}$, apoA-I$^{-/-}$ mice. A–D: Oil Red O-stained liver sections. A, B: Liver sections from 2 week 0.1% cholesterol + 10% palm oil-fed LDLr$^{-/-}$, apoA-I$^{-/-}$ and LDLr$^{-/-}$ mice, respectively. C, D: Liver sections from 16 week 0.1% cholesterol + 10% palm oil-fed LDLr$^{-/-}$, apoA-I$^{-/-}$ and LDLr$^{-/-}$ mice, respectively. Magnification, ×10. E: Time-dependent change in total liver cholesterol mass expressed as µg total cholesterol/mg wet weight (w wt). Liver wet weights were not different between genotypes at any time point. Note that smaller lipid droplets in LDLr$^{-/-}$, apoA-I$^{-/-}$ compared with LDLr$^{-/-}$ mice at 16 weeks are consistent with the 5-fold lower liver cholesterol content. These droplets likely represent droplets of cholesteryl ester, because liver triglyceride levels were similar between genotypes. Asterisks indicate statistically significant differences at $P < 0.02$ comparing liver cholesterol content in LDLr$^{-/-}$, apoA-I$^{-/-}$ versus LDLr$^{-/-}$ mice. All values represent means ± SD for each genotype for eight male and eight female mice. No statistically significant differences in hepatic cholesterol content were noted between mice of different genders. The hepatic free cholesterol-to-total cholesterol ratio was similar for all groups at all times. Similar changes in liver cholesterol were also seen when fed a 0.1% cholesterol + 10% safflower diet for the same length of time.

cumulation. Skin sections were subjected to immunohistochemical analysis for the presence of the mouse macrophage-specific antigen F4/80; the results are shown in **Fig. 7**. Skin sections from diet-fed LDLr$^{-/-}$ mice, shown in Fig. 7A, had little staining for F4/80 (reddish-brown), whereas sections from LDLr$^{-/-}$, apoA-I$^{-/-}$ mice, shown in Fig. 7B, fed 0.1% cholesterol + 10% palm oil for 16 weeks show extensive infiltration of macrophages into the skin. Thus, these data suggest that the dermal thickening in the diet-fed LDLr$^{-/-}$, apoA-I$^{-/-}$ mouse skin was a direct consequence of cholesterol and macrophage infiltration.

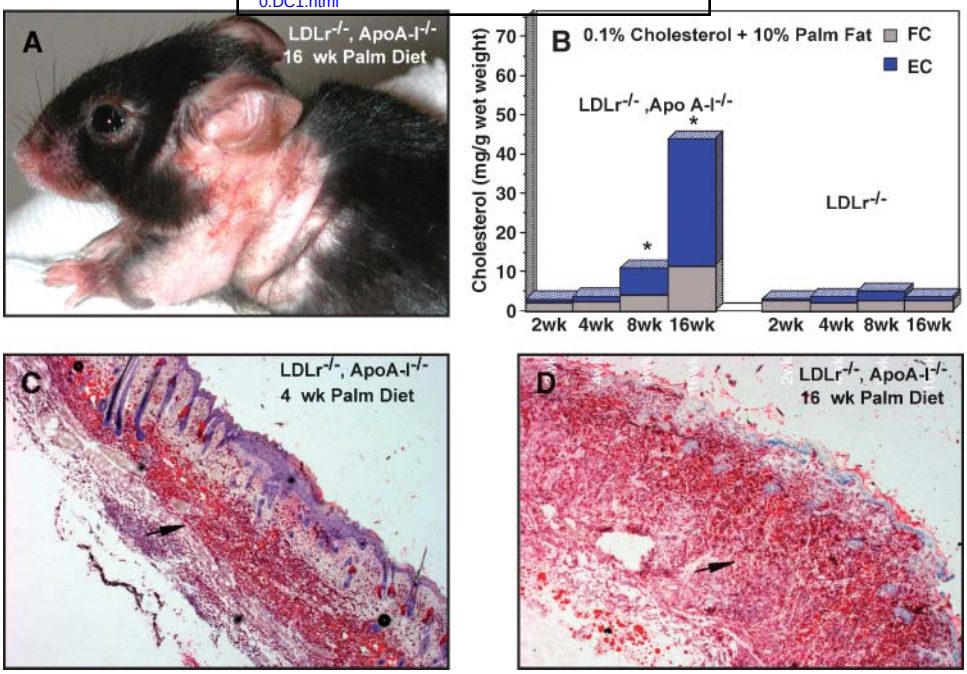

Fig. 6. Time course increase in skin cholesterol mass in LDLr$^{-/-}$, apoA-I$^{-/-}$ and LDLr$^{-/-}$ mice. A: Skin fold thickening associated with cholesterol accumulation in LDLr$^{-/-}$, apoA-I$^{-/-}$ mice fed a 0.1% cholesterol + 10% palm oil diet for 12–16 weeks. B: Skin free cholesterol (FC) and ester cholesterol (EC) mass determined by GC from LDLr$^{-/-}$, apoA-I$^{-/-}$ and LDLr$^{-/-}$ mice as a function of time on diet. No regional differences in skin cholesterol content were noted when four distinct regions were assayed independently. Asterisks indicate statistically significant differences at $P < 0.01$ comparing skin total cholesterol in LDLr$^{-/-}$, apoA-I$^{-/-}$ versus LDLr$^{-/-}$ mice. All values represent means for each genotype of six male and six female mice. C: Oil Red O-stained sections of skin from LDLr$^{-/-}$, apoA-I$^{-/-}$ mice after 4 weeks of diet localized mainly in the dermis. D: Oil Red O staining in skin sections from LDLr$^{-/-}$, apoA-I$^{-/-}$ mice after 16 weeks on diet. Arrows indicate dermal regions of dense lipid staining from 4 week diet-fed mouse skin, which thickens progressively to the dramatic staining seen in skin from 16 week diet-fed LDLr$^{-/-}$, apoA-I$^{-/-}$ mice. Magnification, ×4.

Cholesterol accumulation is associated with cellular inflammation after 4 weeks of diet

Based on the increase in skin cholesterol after ~4 weeks of diet (Fig. 6B, C), we examined the relative mRNA levels for a number of genes controlling cholesterol synthesis, cellular inflammation, and receptor expression. As shown in **Fig. 8A**, the relative mRNA abundance for a number of genes was statistically different between 4 week diet-fed LDLr$^{-/-}$, apoA-I$^{-/-}$ and LDLr$^{-/-}$ mice. In contrast, this was not the case for liver mRNA expression in the same 4 week diet-fed LDLr$^{-/-}$, apoA-I$^{-/-}$ and LDLr$^{-/-}$ mice (Fig. 8B). On examination of the mRNA levels affected in the skin of 4 week diet-fed LDLr$^{-/-}$, apoA-I$^{-/-}$ mice, both HMG-CoA reductase and sterol-regulatory element binding protein-1c were reduced by ~2-fold relative to LDLr$^{-/-}$ mice. Protein markers of inflammation, such as serum amyloid-P component, tumor necrosis factor-α, langerin (a marker for Langerhans cells), and cyclooxygenase-2, were all increased significantly in LDLr$^{-/-}$, apoA-I$^{-/-}$ mouse skin. Interestingly, of the receptors examined, CD-36, LDL receptor-like protein, and scavenger receptor-A type 1 were all reduced significantly in LDLr$^{-/-}$, apoA-I$^{-/-}$ mouse skin, whereas the lectin-like oxidized low density lipoprotein receptor (LOX-1) mRNA showed a significant increase in mRNA expression level.

Cholesterol mass in resident and elicited peritoneal macrophages

A fundamental question regarding the origin of the massive macrophage infiltration into the skin lead to an evaluation of the cholesterol content in circulating monocyte-macrophages derived from 16 week chow- and diet-fed LDLr$^{-/-}$, apoA-I$^{-/-}$ and LDLr$^{-/-}$ mice. In these experiments, both resident and elicited peritoneal macrophages were analyzed for their free and esterified cholesterol content, as shown in **Fig. 9A** for resident peritoneal macrophages and Fig. 9B for thioglycollate-elicited peritoneal macrophages. On the chow diet, resident peritoneal macrophages from both LDLr$^{-/-}$, apoA-I$^{-/-}$ and LDLr$^{-/-}$ mice showed similar levels of free cholesterol, averaging ~15–18 μg/mg cell protein (Fig. 9A). When mice were challenged with the 0.1% cholesterol + 10% palm oil diet for 16 weeks, both genotypes showed an increase in free and esterified cholesterol. Comparatively, however, the diet-fed LDLr$^{-/-}$ mice showed a 1.5- to 2-fold higher content of free and esterified cholesterol compared with LDLr$^{-/-}$, apoA-I$^{-/-}$ mice. This difference in resident macrophage cholesterol content between the two diet-fed genotypes was highly reflective of the ~2-fold difference observed in the total

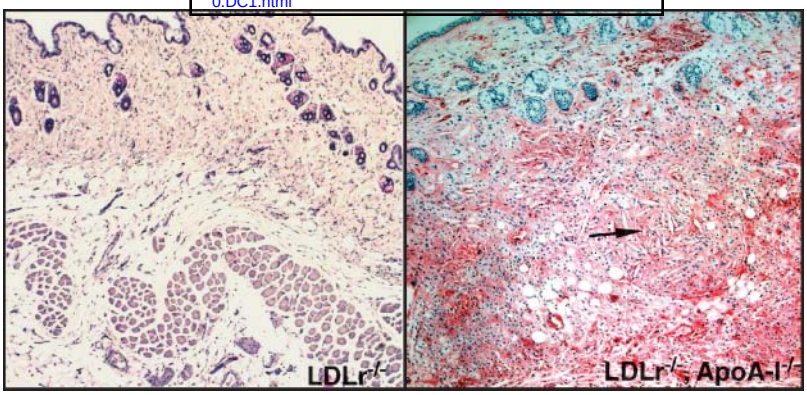

Fig. 7. Immunohistochemical detection of macrophage F4/80 in skin of LDLr$^{-/-}$, apoA-I$^{-/-}$ mice. Skin sections from LDLr$^{-/-}$ (left) and LDLr$^{-/-}$, apoA-I$^{-/-}$ (right) mice fed a 0.1% cholesterol + 10% palm oil diet for 16 weeks show major differences in the extent of dermal macrophage foam cell accumulation. The presence of mouse macrophage F4/80 antigen shows darker red staining in the LDLr$^{-/-}$, apoA-I$^{-/-}$ section than that seen in LDLr$^{-/-}$ mouse skin. Cholesterol clefts (arrow) can also be seen within the regions containing massive foam cell accumulation in LDLr$^{-/-}$, apoA-I$^{-/-}$. Magnification, ×10.

plasma cholesterol when the two diet-fed genotypes were compared (Fig. 1).

The cholesterol content from elicited peritoneal macrophages (Fig. 9B) shows a very similar trend to that seen for the resident peritoneal macrophages, with the exception that the levels of free and esterified cholesterol were 2- to 3-fold higher in all cases than in resident macrophages. Again, when both genotypes were fed chow for 16 weeks, their elicited peritoneal macrophage cholesterol content was similar, reflecting to some degree the similarity in total plasma cholesterol concentrations (Fig. 1), but yet overall higher in cholesterol content than the resident peritoneal macrophages.

When mice were fed diet for 16 weeks and their elicited macrophages isolated, the same genotypic difference in cholesterol mass was seen between LDLr$^{-/-}$, apoA-I$^{-/-}$ and LDLr$^{-/-}$ mice as was seen in the resident peritoneal macrophages, with the exception of the magnitude of cholesterol mass. In the elicited peritoneal macrophages, the esterified cholesterol content was nearly 50–60% of the total cholesterol mass for both genotypes, with the LDLr$^{-/-}$ mice again showing an ~2-fold greater total content of cholesterol than diet-fed LDLr$^{-/-}$, apoA-I$^{-/-}$ mice.

Skin cholesterol accumulation leads to systemic inflammation

To examine other changes in lipid composition associated with the increase in skin cholesterol mass, the phospholipid fatty acid composition was evaluated in diet-fed LDLr$^{-/-}$, apoA-I$^{-/-}$ mice. **Figure 10** shows the percentage of arachidonic acid (20:4) and linoleic acid (18:2) in skin phospholipid over the course of the 16 week diet study. After 4 weeks of diet, the LDLr$^{-/-}$, apoA-I$^{-/-}$ mice showed a statistically significant increase in the percentage of 20:4 in phospholipid compared with LDLr$^{-/-}$ mice. The percentage of 20:4 in the skin continued to increase with time on diet in LDLr$^{-/-}$, apoA-I$^{-/-}$ mice. This increase in 20:4 was in contrast to that of 18:2, which did not show any difference between genotypes at any other times after the switch from chow to the experimental diet. Because arachidonic acid is a well-established precursor for the synthesis of inflammatory lipid mediators, these data support the idea that inflammation in the skin occurs as early as 4 weeks after starting the diet and correlates with the mass influx of cholesterol in this tissue.

Of all the bioactive lipid mediators of inflammation, among the most highly potent are the isoprostanes produced from the free radical-catalyzed reaction of polyunsaturated fatty acids. In particular, the F_2-α isomers are derived from arachidonic acid. Thus, given the increase in 20:4 in mouse skin, we next determined the content of skin F_2-isoprostane after 16 weeks of diet. Here, we found that LDLr$^{-/-}$, apoA-I$^{-/-}$ mice had ~3-fold greater amounts of isoprostanes in skin than LDLr$^{-/-}$ mice, with values of 9.0 ± 0.9 and 3.5 ± 0.5 ng/mg protein, respectively (data not shown).

Further lipid analyses by mass spectrometry revealed enrichment in sphingomylein content in diet-fed LDLr$^{-/-}$, apoA-I$^{-/-}$ mouse skin. The results shown in **Fig. 11** indicate a 6- to 8-fold greater mass of sphingomylein in 16 week diet-fed LDLr$^{-/-}$, apoA-I$^{-/-}$ mice (Fig. 11A) than in LDLr$^{-/-}$ mice (Fig. 11B). In each panel, arrows indicate the mass/charge ions for sphingomyelin, which showed a large difference between genotypes fed diet for 16 weeks.

Rodent skin has been shown to contain a number of related sterol derivatives, with cholesterol being the most abundant (38). To examine the sterol distribution in the skin of diet-fed LDLr$^{-/-}$, apoA-I$^{-/-}$ and LDLr$^{-/-}$ mice, mass spectrometric analyses were conducted on skin lipid extracts. From skin of 16 week diet-fed LDLr$^{-/-}$ mice, cholesterol (Δ^5-cholestenol) and lathosterol (Δ^7-cholestenol) accounted for >70% of the sterol extracted. In contrast, from 16 week diet-fed LDLr$^{-/-}$, apoA-I$^{-/-}$ mice, >90% of the sterol was in the form of cholesterol. These data suggest that the accumulation of skin cholesterol was likely via lipoproteins and ultimately derived from the cholesterol contained in the diet.

The systemic inflammation associated with the accumulation of cholesterol in the skin of diet-fed LDLr$^{-/-}$,

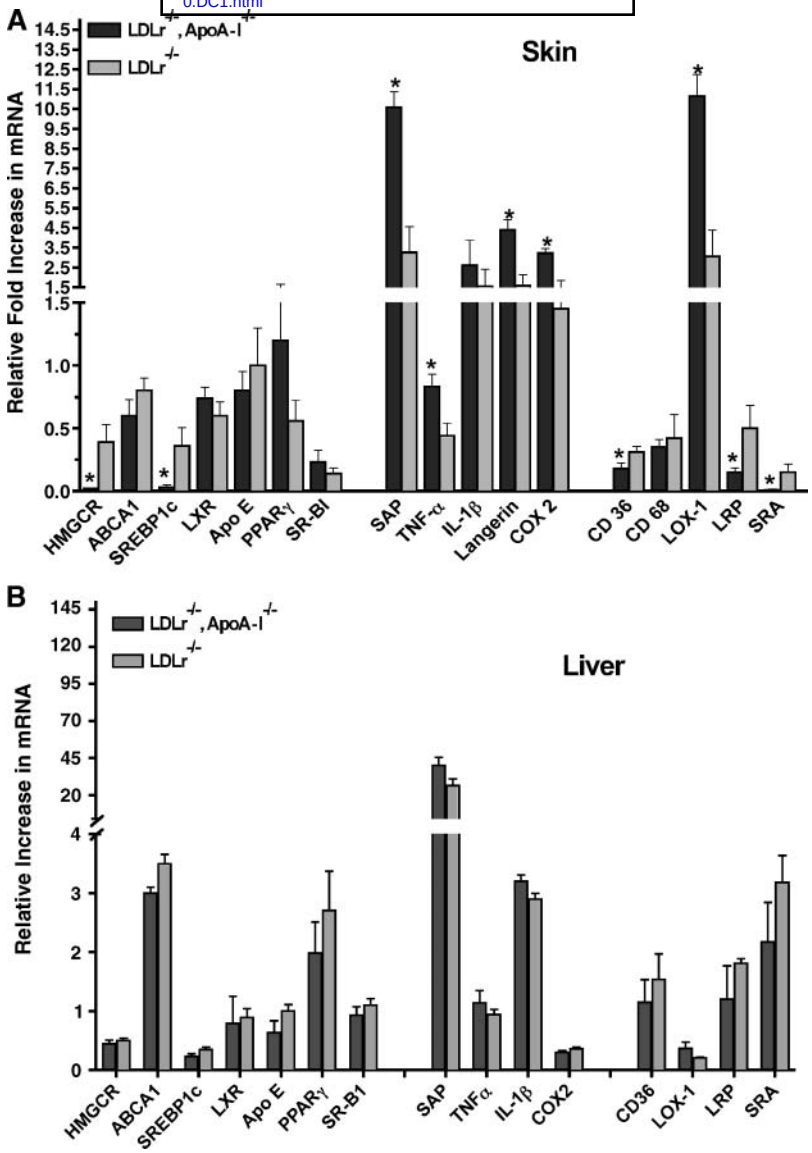

Fig. 8. Relative mRNA abundance in liver and skin of LDLr$^{-/-}$, apoA-I$^{-/-}$ and LDLr$^{-/-}$ mice fed a 0.1% cholesterol + 10% palm oil diet for 4 weeks. Sections of liver and skin were used for RNA isolation, cDNA synthesis, and RT-PCR analyses using panels of primers for the detection of expression levels of genes involved in cholesterol homeostasis, inflammation, and receptor mRNAs. Relative mRNA fold differences are shown in A for liver and in B for skin. All values represent means ± SD from four to eight individual mice. Asterisks indicate statistically significant differences at $P < 0.05$ between mRNA levels for LDLr$^{-/-}$, apoA-I$^{-/-}$ versus LDLr$^{-/-}$ mice. HMGCR, 3-hydroxy-3-methylglutaryl-coenzyme A reductase; SREBP1c, sterol-regulatory element binding protein-1c; LXR, liver X receptor; PPARγ, peroxisome proliferator-activated receptor γ; SR-BI, scavenger receptor class B type I; SAP, Serum amyloid P component; TNF-α, tumor necrosis factor-α; IL-1β, interleukin-1β; COX-2, cyclooxygenase-2; LOX-1, lectin-like oxidized low density lipoprotein receptor; LRP, LDL receptor-like protein; SRA, scavenger receptor-A type 1.

apoA-I$^{-/-}$ mice was also marked by an increase in plasma serum amyloid A levels, a marker of inflammation (**Table 1**). Plasma serum amyloid A levels were measured at 2, 4, 8, 12, and 16 weeks (data shown for 16 weeks only) after initiating the diet. However, only at 12 and 16 weeks were the plasma serum amyloid A values statistically different between diet-fed LDLr$^{-/-}$, apoA-I$^{-/-}$ and LDLr$^{-/-}$ mice. These results suggest that the massive accumulation of skin cholesterol and the associated cutaneous xanthomatosis and pruritus were likely responsible for triggering a systemic inflammatory state in these mice. The consumption of dietary fat and cholesterol in LDLr$^{-/-}$, apoA-I$^{-/-}$ mice was also found to induce MCP-1 protein levels (Table 1).

DISCUSSION

LDLr$^{-/-}$, apoA-I$^{-/-}$ and LDLr$^{-/-}$ mice fed 0.1% cholesterol and 10% palm oil showed an ~2.5-fold lower total plasma cholesterol concentration than LDLr$^{-/-}$ mice. Despite the lower plasma VLDL and LDL concentrations, diet-fed LDLr$^{-/-}$, apoA-I$^{-/-}$ mice accumulated

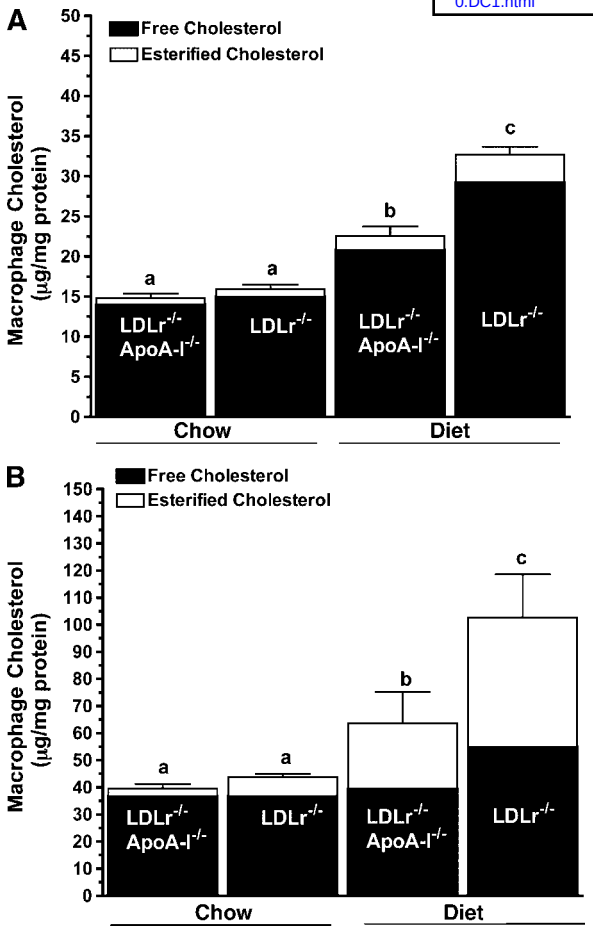

Fig. 9. Free and esterified cholesterol mass in resident peritoneal macrophages (A) and from thioglycollate-elicited peritoneal macrophages (B). All macrophages were isolated from LDLr$^{-/-}$, apoA-I$^{-/-}$ and LDLr$^{-/-}$ mice fed a 0.1% cholesterol + 10% palm oil diet or a chow diet for 16 weeks. Cholesterol mass was measured in diet-fed mouse peritoneal macrophages as described in Materials and Methods. All values represent means ± SD of three to five male mice. Significant differences at $P < 0.05$ are indicated by unlike letters.

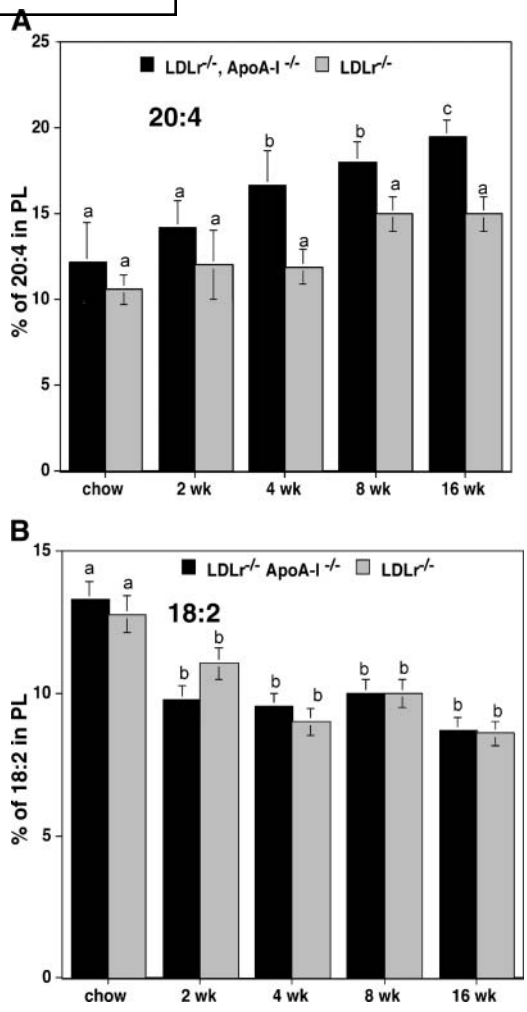

Fig. 10. Distribution of phospholipid (PL) arachidonic acid (20:4) and linoleic acid (18:2) in mouse skin. Diet-fed LDLr$^{-/-}$, apoA-I$^{-/-}$ and LDLr$^{-/-}$ mice were fed 0.1% cholesterol + 10% palm oil for 2, 4, 8, and 16 weeks or chow for 16 weeks. At the time of necropsy, matched regions of skin were extracted and the phospholipid fraction was isolated. The fatty acid content was determined by GC on four to six individual animals per genotype. The arachidonic acid phospholipid content was significantly different at $P < 0.002$ for LDLr$^{-/-}$, apoA-I$^{-/-}$ versus LDLr$^{-/-}$ mice at 4, 8, and 16 weeks of diet, as indicated by the unlike letters. All values represent means ± SD.

more than double the mass of total body cholesterol than LDLr$^{-/-}$ mice. Surprisingly, the accumulation of cholesterol occurred predominantly in the skin of the double knockout mice and not to any significant extent in any other major organs studied. A massive accumulation of cholesterol in the skin of diet-fed mice has been reported previously for a number of mouse genotypes, most notably the diet-fed apoE knockout (39, 40) and ACAT1$^{-/-}$, apoE$^{-/-}$ and ACAT1$^{-/-}$, LDLr$^{-/-}$ double knockout mouse models (41, 42). Similar to our studies, reports from diet-fed ABCA1$^{-/-}$, LDLr$^{-/-}$ and ABCA1$^{-/-}$, apoE$^{-/-}$ (43–45) double knockout mice have shown massive cholesterol accumulation in the skin, despite a relatively modest plasma cholesterol level (~500–600 mg/dl). In these studies, the skin was the predominant site of cholesterol accumulation, whereas the uterus, stomach, lymph nodes, kidney, and lung were also found to be cholesterol-enriched by histological examination. No data were provided on changes in liver cholesterol content in diet-fed ABCA1$^{-/-}$, LDLr$^{-/-}$ and ABCA1$^{-/-}$, apoE$^{-/-}$ mice (44). Thus, one common feature that all of these mouse models share, which also appears to relate to the massive accumulation of cholesterol in the skin, is that of deficits in genes regulating cholesterol homeostasis (i.e., LDLr, ABCA1, apoE, and apoA-I).

Although it might be reasonable to hypothesize that because diet-fed LDLr$^{-/-}$, apoA-I$^{-/-}$ mice lack plasma HDL apoA-I, a continual accumulation of skin cholesterol represents a defect in the reverse cholesterol transport pathway. Following this reasoning, one might consider that the reported 2- to 3-fold increase in apoE levels in LDLr$^{-/-}$, apoA-I versus LDLr$^{-/-}$ mice (17, 46) contributes to an increased uptake by skin LDL-related receptors and thus assists in the accumulation of cholesterol in the skin. However, several lines of evidence suggest that the mechanism of cholesterol accumulation in the skin may be

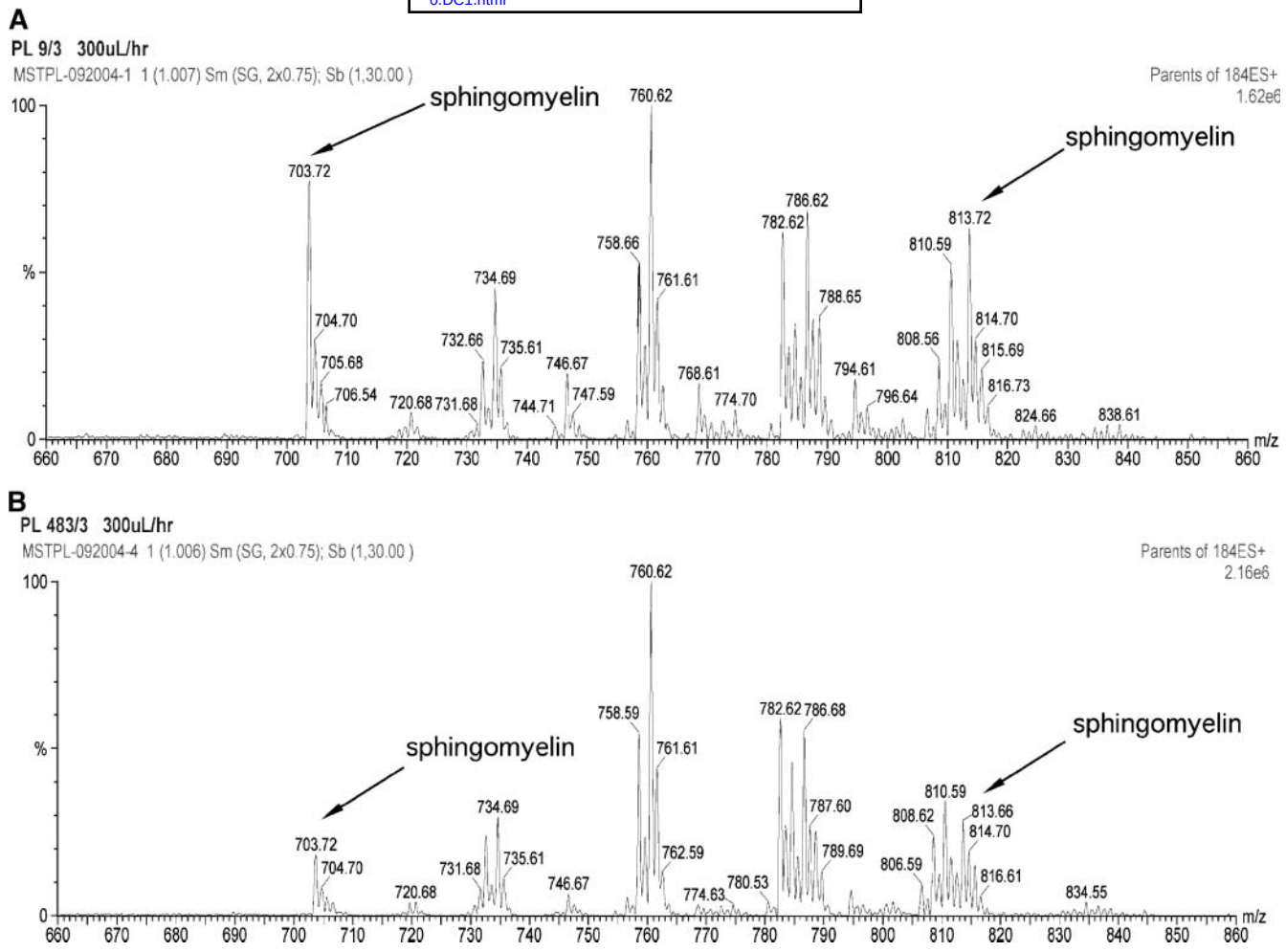

Fig. 11. Mass spectrometric analysis of phospholipids extracted from the skin of 16 week diet-fed LDLr$^{-/-}$, apoA-I$^{-/-}$ and LDLr$^{-/-}$ mice. Arrows indicate signature mass-to-charge (*m/z*) ions for sphingomyelin. A: Two *m/z* ions for sphingomyelin extracted from 16 week diet-fed LDLr$^{-/-}$, apoA-I$^{-/-}$ mice. B: Intensity for the same *m/z* ions from the skin phospholipids of 16 week diet-fed LDLr$^{-/-}$ mice.

more complex. The first and most difficult fact to reconcile with a "defective reverse cholesterol transport mechanism" is that only the skin appears to accumulate massive amounts of cholesterol in response to the dietary challenge in LDLr$^{-/-}$, apoA-I$^{-/-}$ mice, whereas many other tissues in the body express LDL-related receptors. In addition, the role of apoE in this process does not appear to be absolute, because a number of reports show similar accumulations of skin cholesterol in the total absence of apoE (37–43).

TABLE 1. Concentration of plasma proteins associated with inflammation in 16 week diet-fed LDLr$^{-/-}$, apoA-I$^{-/-}$ and LDLr$^{-/-}$ mice

Genotype	Serum Amyloid A	MCP-1 Protein
	μg/ml@pg/ml	
LDLr$^{-/-}$ apoA-I$^{-/-}$ (n = 5)	9.8 ± 1.0^a	175 ± 26^a
LDLr$^{-/-}$ (n = 5)	3.3 ± 0.5^b	83 ± 10^b

LDLr$^{-/-}$ apoA-I$^{-/-}$, low density lipoprotein receptor-deficient/apolipoprotein A-I-deficient; MCP-1, Monocyte chemotactic protein-1. Plasma concentrations for serum amyloid A and MCP-1 were determined as described in Materials and Methods. All values represent means ± SD of five mice. No differences in plasma MCP-1 were seen between genotypes fed chow for 16 weeks (60.3 ± 8 and 71.5 ± 5.7 pg/ml for LDLr$^{-/-}$apoA-I$^{-/-}$ and LDLr$^{-/-}$ mice, respectively). Likewise, no differences in plasma serum amyloid A were seen between genotypes fed chow for 16 weeks (0.29 ± 0.06 and 0.19 ± 0.09 μg/ml for LDLr$^{-/-}$apoA-I$^{-/-}$ and LDLr$^{-/-}$ mice, respectively). Unlike superscripts indicate statistically significant differences at $P < 0.05$.

An alternative explanation for the massive accumulation of skin cholesterol may be related to reports of altered dendritic cell mobilization in apoE$^{-/-}$ and LDLr$^{-/-}$ mice (47, 48). Dendritic cells are major antigen-presenting cells that typically reside in the periphery, continuously migrating to lymph nodes and promoting peripheral tolerance (49). Immature dendritic cells sense the presence of an infectious agent and mature, allowing the expression of cytokines, which activate the immune system and thus adaptive immune responses (50). The balance in dendritic cell activation and migration is critical in maintaining self-tolerance (51). Because the skin is a major target organ for many autoimmune diseases, dendritic cell function was studied in C57BL/6 apoE or LDLr knockout mice maintained on diet for 10–28 weeks (47, 48). Although in these studies, mass accumulation of cholesterol in the skin was not present (as in our diet-fed LDLr$^{-/-}$ mice), it was reported that ~50% fewer skin-specific dendritic cells, also

called Langerhans cells, were present in skin draining lymph nodes by 16 weeks and were shown to remain in the epidermis in an activated form. Thus, abnormal dendritic cell migration leads to dermal thickening, inflammation, and suppressed immune priming. Interestingly, dendritic cell migration was restored by the addition of HDL or HDL-associated platelet-activating factor acetylhydrolase.

The connection between skin dendritic cell mobilization and cholesterol homeostasis appears to be significant. The massive accumulation of skin cholesterol seen in our studies using diet-fed LDLr$^{-/-}$, apoA-I$^{-/-}$ mice as well as in other hypercholesterolemic mouse models may represent an extreme or enhanced version of the dendritic cell dysfunction reported in chow- and diet-fed apoE and LDLr knockout mice, as outlined above (45, 46). In support of this mechanism, we measured langerin mRNA levels in skin. At 4 weeks after initiating the diet, similar in time to when mass amounts of cholesterol accumulated in the skin, langerin mRNA levels were increased significantly in LDLr$^{-/-}$, apoA-I$^{-/-}$ compared with LDLr$^{-/-}$ mice. Interestingly, both skin HMG-CoA reductase and sterol-regulatory element binding protein-1c mRNA were down-regulated in LDLr$^{-/-}$, apoA-I$^{-/-}$ mice at 4 weeks. These results strongly suggest that the combination of hypercholesterolemia, cholesterol imbalance, and dendritic cell function is the basis for this profound phenotype; thus, a connection between cholesterol homeostasis and self-tolerance is suggestive.

Also consistent with this hypothesis is the significant increase in skin tumor necrosis factor-α, Serum amyloid P component, and cyclooxygenase-2 mRNA levels in LDLr$^{-/-}$, apoA-I$^{-/-}$ mice as early as 4 weeks after starting the diet. Additionally, these markers of local inflammation correlate with the increase in phospholipid 20:4 and isoprostane levels in the skin of LDLr$^{-/-}$, apoA-I$^{-/-}$ mice. In studies of dendritic cell function (45, 46), it is interesting that dendritic cell mobilization was restored when HDL or platelet-activating factor acetylhydrolase was infused into the apoE knockout mice, suggesting that the accumulation of oxidized phospholipid or its metabolites contributes to the dendritic cell dysfunction in the skin.

In addition to the connection between cholesterol balance, inflammation, and dendritic cell mobility, there is also growing interest in the link between T-cell cytokine production, pruritus (itching), and atopic skin inflammation (e.g., atopic dermatitis) (52). In the current studies, diet-fed LDLr$^{-/-}$, apoA-I$^{-/-}$ mice showed severe pruritus starting as early as 10–12 weeks after starting the diet, correlating with an increase in skin sphingomyelin content. In humans, "itching" has been linked to the loss of barrier function in the skin, which is believed to be controlled in part by the amount of ceramides and sphingomyelin in the stratum corneum (53, 54). The level of skin ceramides has also been linked to the control of human dendritic cell survival (55), which in turn affects the activation and regulation of the immune response. Together, these concepts suggest that cellular cholesterol balance is an important consideration when linking immune response and inflammatory skin disorders.

In summary, we believe that further study in hypercholesterolemic LDLr$^{-/-}$, apoA-I$^{-/-}$ mice will promote a broader mechanistic understanding of the interrelationships between cellular cholesterol balance, inflammation, and immune function.

The authors gratefully acknowledge Dr. Richard St. Clair and Ms. Katrina Rankin for technical advice on performing cholesterol measurements on elicited and resident mouse peritoneal macrophages. The authors also thank Ms. Tara Loughlin, Persida Tahiri, Hermina Borgerink, and Janet Sawyer and Drs. Martha Wilson and Llijun Tang for their expert technical assistance. The authors thank Dr. Steve Turley for his suggestion of conducting whole body cholesterol measurements. These studies were supported by grants from the National Heart, Lung, and Blood Institute, National Institutes of Health (HL-49373 and HL-64163 to M.G.S.-T.).

REFERENCES

1. Gordon, D. J., J. L. Probstfield, R. J. Garrison, J. D. Neaton, W. P. Castelli, J. D. Knoke, D. R. J. Jacobs, S. Bangdiwala, and H. A. Tyroler. 1989. High-density lipoprotein cholesterol and cardiovascular disease. Four prospective American studies. *Circulation.* **79:** 8–15.
2. Glomset, J. A., and K. R. Norum. 1973. The metabolic role of lecithin:cholesterol acyltransferase: perspective from pathology. *Adv. Lipid Res.* **1:** 1–65.
3. Fielding, C. J., and P. E. Fielding. 1995. Molecular physiology of reverse cholesterol transport. *J. Lipid Res.* **36:** 211–228.
4. Spady, D. K., L. A. Woollett, R. S. Meidell, and H. H. Hobbs. 1998. Kinetic characteristics and regulation of HDL cholesteryl ester and apolipoprotein transport in the apoA-I$^{-/-}$ mouse. *J. Lipid Res.* **39:** 1483–1492.
5. Stein, O., Y. Dabach, G. Hollander, M. Ben-Naim, G. Halperin, and Y. Stein. 1999. High levels of human apolipoprotein A-I and high density lipoproteins in transgenic mice do not enhance efflux of cholesterol from a depot of injected lipoproteins. Relevance to regression of atherosclerosis? *Atherosclerosis.* **144:** 367–374.
6. Alam, K., R. S. Meidell, and D. K. Spady. 2001. Effect of up-regulating individual steps in the reverse cholesterol transport pathway on reverse cholesterol transport in normolipidemic mice. *J. Biol. Chem.* **276:** 15641–15649.
7. Jolley, C. D., L. A. Woollett, S. D. Turley, and J. M. Dietschy. 1998. Centripetal cholesterol flux to the liver is dictated by events in the peripheral organs and not by the plasma high density lipoprotein or apolipoprotein A-I concentration. *J. Lipid Res.* **39:** 2143–2149.
8. Dansky, H. M., S. A. Charlton, C. B. Barlow, M. Tamminen, J. D. Smith, J. S. Frank, and J. L. Breslow. 1999. Apo A-I inhibits foam cell formation in apo E-deficient mice after monocyte adherence to endothelium. *J. Clin. Invest.* **104:** 31–39.
9. Boisvert, W. A., A. S. Black, and L. K. Curtiss. 1999. ApoA1 reduces free cholesterol accumulation in atherosclerotic lesions of apoE-deficient mice transplanted with apoE-expressing macrophages. *Arterioscler. Thromb. Vasc. Biol.* **19:** 525–530.
10. Zhang, Y., I. Zanotti, M. P. Reilly, J. M. Glick, G. H. Rothblat, and D. J. Rader. 2003. Overexpression of apolipoprotein A-I promotes reverse transport of cholesterol from macrophages to feces in vivo. *Circulation.* **108:** 661–663.
11. Zhang, Y., J. R. Da Silva, M. Reilly, J. T. Billheimer, G. H. Rothblat, and D. J. Rader. 2005. Hepatic expression of scavenger receptor class B type I (SR-BI) is a positive regulator of macrophage reverse cholesterol transport in vivo. *J. Clin. Invest.* **115:** 2870–2874.
12. Tall, A. R., N. Wang, and P. Mucksavage. 2001. Is it time to modify the reverse cholesterol transport model? *J. Clin. Invest.* **108:** 1273–1275.
13. Rader, D. J., and E. Pure. 2005. Lipoproteins, macrophage function, and atherosclerosis: beyond the foam cell? *Cell Metab.* **1:** 223–230.

14. Libby, P. 2001. Managing the risk of atherosclerosis: the role of high-density lipoprotein. *Am. J. Cardiol.* **88:** 3N–8N.
15. Steinberg, D. 2002. Atherogenesis in perspective: hypercholesterolemia and inflammation as partners in crime. *Nat. Med.* **8:** 1211–1217.
16. Navab, M., S. Y. Hama, C. J. Cooke, G. M. Anantharamaiah, M. Chaddha, L. Jin, G. Subbanagounder, K. F. Faull, S. T. Reddy, N. E. Miller, et al. 2000. Normal high density lipoprotein inhibits three steps in the formation of mildly oxidized low density lipoprotein: step 1. *J. Lipid Res.* **41:** 1481–1494.
17. Zabalawi, M., S. Bhat, T. Loughlin, M. J. Thomas, E. Alexander, M. Cline, B. Bullock, M. Willingham, and M. G. Sorci-Thomas. 2003. Induction of fatal inflammation in LDL receptor and apoA-I double-knockout mice fed dietary fat and cholesterol. *Am. J. Pathol.* **163:** 1201–1213.
18. Moore, R. E., M. A. Kawashiri, K. Kitajima, A. Secreto, J. S. Millar, D. Pratico, and D. J. Rader. 2003. Apolipoprotein A-I deficiency results in markedly increased atherosclerosis in mice lacking the LDL receptor. *Arterioscler. Thromb. Vasc. Biol.* **23:** 1914–1920.
19. Moore, R. E., M. Navab, J. S. Millar, F. Zimetti, S. Hama, G. H. Rothblat, and D. J. Rader. 2005. Increased atherosclerosis in mice lacking apolipoprotein A-I attributable to both impaired reverse cholesterol transport and increased inflammation. *Circ. Res.* **97:** 763–771.
20. Rudel, L. L., K. Kelley, J. K. Sawyer, R. Shah, and M. D. Wilson. 1998. Dietary monounsaturated fatty acids promote aortic atherosclerosis in LDL receptor-null, human apoB100-overexpression transgenic mice. *Arterioscler. Thromb. Vasc. Biol.* **18:** 1818–1827.
21. Furbee, J. W., Jr., J. K. Sawyer, and J. S. Parks. 2002. Lecithin: cholesterol acyltransferase (LCAT) deficiency increases atherosclerosis in the low density lipoprotein receptor and apolipoprotein E knockout mice. *J. Biol. Chem.* **277:** 3511–3519.
22. Schwarz, M., D. W. Russell, J. M. Dietschy, and S. D. Turley. 1998. Marked reduction in bile acid synthesis in cholesterol 7alpha-hydroxylase-deficient mice does not lead to diminished tissue cholesterol turnover or to hypercholesterolemia. *J. Lipid Res.* **39:** 1833–1843.
23. Parks, J. S., F. L. Johnson, M. D. Wilson, and L. L. Rudel. 1990. Effect of fish oil diet on hepatic lipid metabolism in nonhuman primates: lowering of secretion of hepatic triglyceride but not apoB. *J. Lipid Res.* **31:** 455–466.
24. Parks, J. S., and B. C. Bullock. 1987. Effect of fish oil versus lard diets on the chemical and physical properties of low density lipoproteins from nonhuman primates. *J. Lipid Res.* **28:** 173–182.
25. DeLong, C. J., P. R. Baker, M. Samuel, Z. Cui, and M. J. Thomas. 2001. Molecular species composition of rat liver phospholipids by ESI-MS/MS: the effect of chromatography. *J. Lipid Res.* **42:** 1959–1968.
26. Thomas, M. J., Q. Chen, M. G. Sorci-Thomas, and L. L. Rudel. 2001. Isoprostane levels in lipids extracted from atherosclerotic arteries of nonhuman primates. *Free Radic. Biol. Med.* **30:** 1337–1346.
27. Yancey, P. G., and R. W. St. Clair. 1992. Cholesterol efflux is defective in macrophages from atherosclerosis-susceptible White Carneau pigeons relative to resistant show racer pigeons. *Arterioscler. Thromb.* **12:** 1291–1304.
28. Nordskog, B. K., J. W. Reagan, Jr., and R. W. St. Clair. 1999. Sterol synthesis is up-regulated in cholesterol-loaded pigeon macrophages during induction of cholesterol efflux. *J. Lipid Res.* **40:** 1806–1817.
29. Turley, S. D., B. P. Daggy, and J. M. Dietschy. 1994. Psyllium augments the cholesterol-lowering action of cholestyramine in hamsters by enhancing sterol loss from the liver. *Gastroenterology.* **107:** 444–452.
30. Turley, S. D., B. P. Daggy, and J. M. Dietschy. 1991. Cholesterol-lowering action of psyllium mucilloid in the hamster: sites and possible mechanisms of action. *Metabolism.* **40:** 1063–1073.
31. Mashige, F., N. Tanaka, A. Maki, S. Kamei, and M. Yamanaka. 1981. Direct spectrophotometry of total bile acids in serum. *Clin. Chem.* **27:** 1352–1356.
32. Livak, K. J., and T. D. Schmittgen. 2001. Analysis of relative gene expression data using real-time quantitative PCR and the 2(-Delta Delta C(T)) method. *Methods.* **25:** 402–408.
33. Xie, C., S. D. Turley, and J. M. Dietschy. 1999. Cholesterol accumulation in tissues of the Niemann-Pick type C mouse is determined by the rate of lipoprotein-cholesterol uptake through the coated-pit pathway in each organ. *Proc. Natl. Acad. Sci. USA.* **96:** 11992–11997.
34. Plump, A. S., S. K. Erickson, W. Weng, J. S. Partin, J. L. Breslow, and D. L. Williams. 1996. Apolipoprotein A-I is required for cholesteryl ester accumulation in steroidogenic cells and for normal adrenal steroid production. *J. Clin. Invest.* **97:** 2660–2671.
35. Gwynne, J. T., and B. Hess. 1980. The role of high density lipoproteins in rat adrenal cholesterol metabolism and steroidogenesis. *J. Biol. Chem.* **255:** 10875–10883.
36. Yu, L., J. Li-Haweeksins, R. E. Hammer, K. E. Berge, J. D. Horton, J. C. Cohen, and H. H. Hobbs. 2002. Overexpression of ABCG5 and ABCG8 promotes biliary cholesterol secretion and reduces fractional absorption of dietary cholesterol. *J. Clin. Invest.* **110:** 671–680.
37. Jolley, C. D., J. M. Dietschy, and S. D. Turley. 1999. Genetic differences in cholesterol absorption in 129/Sv and C57BL/6 mice: effect on cholesterol responsiveness. *Am. J. Physiol.* **276:** G1117–G1124.
38. Clayton, R. B., A. N. Nelson, and I. D. Frantz, Jr. 1963. The skin sterols of normal and triparanol-treated rats. *J. Lipid Res.* **4:** 166–176.
39. Feingold, K. R., P. M. Elias, M. Mao-Qiang, M. Fartasch, S. H. Zhang, and N. Maeda. 1995. Apolipoprotein E deficiency leads to cutaneous foam cell formation in mice. *J. Invest. Dermatol.* **104:** 246–250.
40. van Ree, J. H., M. J. Gijbels, W. J. van den Broek, M. H. Hofker, and L. M. Havekes. 1995. Atypical xanthomatosis in apolipoprotein E-deficient mice after cholesterol feeding. *Atherosclerosis.* **112:** 237–243.
41. Accad, M., S. J. Smith, D. L. Newland, D. A. Sanan, L. E. King, Jr., M. F. Linton, S. Fazio, and R. V. Farese, Jr. 2000. Massive xanthomatosis and altered composition of atherosclerotic lesions in hyperlipidemic mice lacking acyl CoA:cholesterol acyltransferase 1. *J. Clin. Invest.* **105:** 711–719.
42. Yagyu, H., T. Kitamine, J. Osuga, R. Tozawa, Z. Chen, Y. Kaji, T. Oka, S. Perrey, Y. Tamura, K. Ohashi, et al. 2000. Absence of ACAT-1 attenuates atherosclerosis but causes dry eye and cutaneous xanthomatosis in mice with congenital hyperlipidemia. *J. Biol. Chem.* **275:** 21324–21330.
43. Aiello, R. J., D. Brees, P. A. Bourassa, L. Royer, S. Lindsey, T. Coskran, M. Haghpassand, and O. L. Francone. 2002. Increased atherosclerosis in hyperlipidemic mice with inactivation of ABCA1 in macrophages. *Arterioscler. Thromb. Vasc. Biol.* **22:** 630–637.
44. Aiello, R. J., D. Brees, and O. L. Francone. 2003. ABCA1-deficient mice: insights into the role of monocyte lipid efflux in HDL formation and inflammation. *Arterioscler. Thromb. Vasc. Biol.* **23:** 972–980.
45. Francone, O. L., L. Royer, G. Boucher, M. Haghpassand, A. Freeman, D. Brees, and R. J. Aiello. 2005. Increased cholesterol deposition, expression of scavenger receptors, and response to chemotactic factors in Abca1-deficient macrophages. *Arterioscler. Thromb. Vasc. Biol.* **25:** 1198–1205.
46. Li, H., R. L. Reddick, and N. Maeda. 1993. Lack of apoA-I is not associated with increased susceptibility to atherosclerosis in mice. *Arterioscler. Thromb.* **13:** 1814–1821.
47. Angeli, V., J. Llodra, J. X. Rong, K. Satoh, S. Ishii, T. Shimizu, E. A. Fisher, and G. J. Randolph. 2004. Dyslipidemia associated with atherosclerotic disease systemically alters dendritic cell mobilization. *Immunity.* **21:** 561–574.
48. Randolph, G. J., V. Angeli, and M. A. Swartz. 2005. Dendritic-cell trafficking to lymph nodes through lymphatic vessels. *Nat. Rev. Immunol.* **5:** 617–628.
49. Reis e Sousa, C. 2004. Activation of dendritic cells: translating innate into adaptive immunity. *Curr. Opin. Immunol.* **16:** 21–25.
50. Rescigno, M. 2002. Dendritic cells and the complexity of microbial infection. *Trends Microbiol.* **10:** 425–461.
51. Palucka, A. K., and J. Banchereau. 2006. Langerhans cells: daughters of monocytes. *Nat. Immunol.* **7:** 223–224.
52. Sonkoly, E., A. Muller, A. I. Lauerma, A. Pivarcsi, H. Soto, L. Kemeny, H. Alenius, M. C. Dieu-Nosjean, S. Meller, J. Rieker, et al. 2006. IL-31: a new link between T cells and pruritus in atopic skin inflammation. *J. Allergy Clin. Immunol.* **117:** 411–417.
53. Okamoto, R., J. Arikawa, M. Ishibashi, M. Kawashima, Y. Takagi, and G. Imokawa. 2003. Sphingosylphosphorylcholine is upregulated in the stratum corneum of patients with atopic dermatitis. *J. Lipid Res.* **44:** 93–102.
54. Jensen, J. M., R. Folster-Holst, A. Baranowsky, M. Schunck, S. Winoto-Morbach, C. Neumann, S. Schutze, and E. Proksch. 2004. Impaired sphingomyelinase activity and epidermal differentiation in atopic dermatitis. *J. Invest. Dermatol.* **122:** 1423–1431.
55. Franchi, L., F. Malisan, B. Tomassini, and R. Testi. 2006. Ceramide catabolism critically controls survival of human dendritic cells. *J. Leukoc. Biol.* **79:** 166–172.